Cerebral Cortex, 2020;00: 1–10

doi: 10.1093/cercor/bhaa098
Original Article

ORIGINAL ARTICLE

Structure–Function Connectomics Reveals Aberrant Developmental Trajectory Occurring at Preadolescence in the Autistic Brain

Changchun He[1,2], Huafu Chen[1,2], Lucina Q. Uddin[3], Asier Erramuzpe[4,5], Paolo Bonifazi[4,6], Xiaonan Guo[1,2], Jinming Xiao[1,2], Heng Chen[7], Xinyue Huang[1,2], Lei Li[1,2], Wei Sheng[1,2], Wei Liao[1,2], Jesus M. Cortes[6,8] and Xujun Duan[1,2]

[1]Department of Life Science and Technology, The clinical Hospital of Chengdu Brain Science Institute, University of Electronic Science and Technology of China, Chengdu 610054, China, [2]MOE Key Lab for Neuroinformation, High-Field Magnetic Resonance Brain Imaging Key Laboratory of Sichuan Province, University of Electronic Science and Technology of China, Chengdu 610054, China, [3]Department of Psychology, University of Miami, Coral Gables, FL 33124, USA, [4]Computational Neuroimaging Laboratory, Biocruces-Bizkaia Health Research Institute, Barakaldo 48903, Spain, [5]Edmond & Lily Safra Center for Brain Sciences, The Hebrew University of Jerusalem, Jerusalem 91905, Israel, [6]Ikerbasque: The Basque Foundation for Science, Bilbao 48013, Spain, [7]School of Medicine, Medical College of Guizhou University, Guiyang 550025, China and [8]Department of Cell Biology and Histology, University of the Basque Country, Leioa, Spain

Address correspondence to Xujun Duan. Email: duanxujun@uestc.edu.cn; Huafu Chen. Email: chenhf@uestc.edu.cn; and Jesus M. Cortes. Email: jesus.m.cortes@gmail.com

Abstract

Accumulating neuroimaging evidence shows that age estimation obtained from brain connectomics reflects the level of brain maturation along with neural development. It is well known that autism spectrum disorder (ASD) alters neurodevelopmental trajectories of brain connectomics, but the precise relationship between chronological age (ChA) and brain connectome age (BCA) during development in ASD has not been addressed. This study uses neuroimaging data collected from 50 individuals with ASD and 47 age- and gender-matched typically developing controls (TDCs; age range: 5–18 years). Both functional and structural connectomics were assessed using resting-state functional magnetic resonance imaging and diffusion tensor imaging data from the Autism Brain Imaging Data Exchange repository. For each participant, BCA was estimated from structure–function connectomics through linear support vector regression. We found that BCA matched well with ChA in TDC children and adolescents, but not in ASD. In particular, our findings revealed that individuals with ASD exhibited accelerated brain maturation in youth, followed by a delay of brain development starting at preadolescence. Our results highlight the critical role of BCA in understanding aberrant developmental trajectories in ASD and provide the new insights into the pathophysiological mechanisms of this disorder.

Key words: autism spectrum disorder, brain connectome age, brain connectivity, diffusion tensor imaging, resting-state functional magnetic resonance imaging

Introduction

Human brain development is a dynamic and complex process involving progressive (e.g., cell growth and myelination) and regressive (e.g., cell death and atrophy) neuronal processes (Silk and Wood 2011). Reflecting the level of brain maturity, individuals with the same chronological age (ChA) might course different trajectories of brain development, as measured by biomarkers of brain anatomy, function, and connectivity across the lifespan (Dosenbach et al. 2010). Such differences reflect both ChA (measured by the time running since birth) and biological age (regardless of birth year, the level of biological maturation at a given time). Previous studies have reported a mismatch between the two ages occurring in parallel with well-established age-related anatomical and functional connectivity variations (Kleinhans et al. 2012; Uddin et al. 2013), consolidating the fact that brain connectivity patterns play an important role in characterizing brain development.

Autism spectrum disorder (ASD) is characterized by impairments of social communication, social reciprocity, and repetitive and stereotyped behaviors and interests (American Psychiatric Association 2013). Recent research has led to the theory of age-related abnormal brain connectivity in ASD (Courchesne et al. 2007; Uddin et al. 2013), showing that functional connectivity (FC) increases in ASD at an early age but abnormally decreases and possibly degenerates in adolescence. Uddin et al. (2013) also suggested that the atypically increased intrinsic FC found in children with ASD may reverse by adulthood. Therefore, it is clear that in ASD the level of brain connectivity abnormalities has a strong dependence on the specific age at which individuals are evaluated (Nomi and Uddin 2015).

Structural neuroimaging has shown a similar pattern in young children with ASD involving widespread increases in fractional anisotropy of white matter tracts (Billeci et al. 2012). Courchesne et al. (2004, 2007) have found that brain development in ASD is characterized by different phases from birth to adulthood, reporting early brain overgrowth at the beginning of life and abnormal slowing of growth in later developmental stages. Taken together, these findings show that patterns of structural connectivity (SC) and FC are associated with abnormal brain development in ASD, and the amount of deviation from normal aging might help with the early detection of clinical outcomes (Ecker et al. 2015). Recently, the process of aging has been assessed through novel computational strategies such as machine learning. Specifically, a new paradigm for brain age estimation has been successfully introduced and applied to different diseases (e.g., Alzheimer's disease and schizophrenia). Brain age estimation has the potential to provide personalized biomarkers of brain development by capturing deviations from typical development based on brain structure and function (Gaser et al. 2013; Schnack et al. 2016; Zimmermann et al. 2016; Liem et al. 2017; Bonifazi et al. 2018). Previous studies have reported that brain age estimation can quantify mismatches between ChA and biological age. In particular, Zimmermann et al. (2016) and Liem et al. (2017) reported that a combination of structural and functional information in brain age estimation can outperform either structural or functional information alone. However, previous studies have reported that structural and functional templates do not correspond to the same physical and physiological mechanisms, despite the fact that brain structure forms the basis of brain function and function exerts the effects on the plasticity of structure (Hermundstad et al. 2013; Diez et al. 2015).

The current study makes the use of the Brain Hierarchical Atlas at the level of 20 module representation, which provides maximum correspondence between structure and function (Diez et al. 2015). We built SC and FC matrices using resting-state functional magnetic resonance imaging (rs-fMRI) and diffusion tensor imaging (DTI) data from the Autism Brain Imaging Data Exchange (ABIDE) database (Di Martino et al. 2014). Based on inter- and intra-module SC and FC matrices, we estimate brain connectome age (BCA) and assess specific patterns of brain developmental trajectories in ASD and typically developing control (TDC). Building upon previous evidence, we hypothesized that brain development in ASD would be accelerated in youth and delayed with increasing age compared with TDC.

Materials and Methods

Participants

Data were selected from the Autism Brain Imaging Data Exchange (ABIDE II) repository (http://fcon_1000.projects.nitrc.org/indi/abide/) (Di Martino et al. 2014, 2017) using strict inclusion criteria (see Supplementary Information for inclusion criteria and diagnosis and clinical assessment details). This selection process resulted in 97 subjects, including 47 TDCs and 50 individuals with ASD from two sites (New York University Langone Medical Center [NYU] and San Diego State University [SDSU]; Table 1).

Neuroimaging Acquisition

MRI data were acquired at NYU with a 3 Tesla Siemens Allegra scanner and at SDSU with a 3 Tesla GE MR750 scanner. The two institutions obtained structural imaging, diffusion imaging, and rs-fMRI (see Supplementary Information for details regarding acquisition parameters).

Image Preprocessing

Diffusion Tensor Imaging

DTI data preprocessing was performed following a similar procedure to previous studies (Bonifazi et al. 2018; Pang et al. 2019). For more details on DTI preprocessing, see Supplementary Information.

The functional partition was generated after applying spatially constrained clustering to the functional data following the procedure in Craddock et al. (2012) and choosing the level of $M = 20$ modules from the Brain Hierarchical Atlas, published in Diez et al. (2015) and available for download at https://www.nitrc.org/projects/biocr_hcatlas/. For each participant, one 2514×2514 SC matrix was obtained (Fig. 1), where the entry (i, j) is given by the mean fractional anisotropy (FA) values along all fibers connecting the two nodes. SC is a symmetric matrix, where connectivity from i to j is equal to that from j to i.

Functional MRI

Functional images were processed with the DPARSF (Yan and Zang 2010) (v4.3.0, http://rfmri.org/DPARSF) software package in MATLAB 2013 (Math Works, Natick, MA). For more details on fMRI preprocessing, see Supplementary Information.

One 2514×2514 FC matrix for each participant was obtained (Fig. 1). Specifically, the element matrix (i, j) of FC was obtained by using the pairwise Pearson correlation coefficient between

Table 1 Participant demographics

Site	Number (n)	Age (mean ± SD)	Gender (M/F)	FIQ (mean ± SD)	MeanFD (mean ± SD)	PST (mean ± SD)	ADOS (mean ± SD)
All sites							
ASD	50	11.3 ± 3.96	43/7	101.1 ± 16.27	0.19 ± 0.10	0.13 ± 0.14	13.5 ± 4.63
TDCs	47	11.3 ± 3.28	45/2	109.3 ± 14.94	0.18 ± 0.13	0.12 ± 0.18	—
P value	—	0.91[a]	0.10[b]	*P* = 0.01[a]	0.82[a]	0.95 [a]	—
NYU							
ASD	22	8.4 ± 2.98	21/1	103.3 ± 18.18	0.22 ± 0.11	0.17 ± 0.16	11.9 ± 4.19
TDCs	23	9.2 ± 1.91	23/0	116.0 ± 14.99	0.20 ± 0.13	0.15 ± 0.18	—
P value	—	0.28[a]	0.30[b]	*P* = 0.01[a]	0.58[a]	0.67 [a]	—
SDSU							
ASD	28	13.5 ± 3.07	22/6	99.4 ± 14.70	0.16 ± 0.09	0.09 ± 0.11	14.8 ± 4.64
TDCs	24	13.4 ± 3.02	22/2	102.8 ± 11.90	0.16 ± 0.12	0.10 ± 0.19	—
P value	—	0.87[a]	0.19[b]	0.36[a]	0.95[a]	0.68 [a]	—

Note: PST, proportion of scrubbed time points (number of "bad" time points/total time points); SD, standard deviation; M, male; F, female; ADOS, total score of the Autism Diagnostic Observation Schedule. "Bad" time points denote time points with frame-wise displacement >0.5 mm, including the preceding time point and the two succeeding time points.
[a]*P* value was obtained by two-sample *t*-test, two-tailed.
[b]*P* value was obtained by Kruskal–Wallis test.

pairs of resting fMRI time series. The correlation coefficients were normalized by the Fisher's *Z* transformation:

$$Z = \frac{1}{2}\sqrt{n-3} \times \ln\left(\frac{1+r}{1-r}\right) \quad (1)$$

where n represents the number of time points and r represents the correlation coefficients between regions of interest (ROIs).

Age Estimation Analysis

Feature Selection

From the original SC and FC matrices for each participant, four different classes of features were generated (Bonifazi et al. 2018): structural internal connectivity (SIC), functional internal connectivity (FIC), structural external connectivity (SEC), and functional external connectivity (FEC, Fig. 1). Given that a module was composed of a set of n ROIs and 20 modules were generated from the 2514 ROIs, each participant had 20×2 [SIC,FIC] and 190 $[20 \times (20–1)/2] \times 2$ (SEC,FEC). After combination of the four classes of features and normalization, the structure–function feature matrix had $N \times 420$ dimensions (N number of individuals times 420 features). To obtain the age-related features, recursive feature elimination with cross-validation (RFECV) was performed (Guyon et al. 2002). In addition, the effect of head motion was controlled for by excluding features that correlated with mean frame-wise displacement (meanFD). As shown in Fig. 1, the feature selection was performed before the cross-validation (see Supplementary Information).

Brain Connectome Age

Linear support vector regression (SVR) is a supervised learning technique based on the concept of support vector machines—used for categorical classification—and generalized for the prediction of continuous variables such as age (Drucker et al. 1997). Of note, SVR has been successfully used in prior studies for assessing brain aging patterns (Dosenbach et al. 2010; Liem et al. 2017). BCA was defined as brain maturation characterized by the brain connectome, and it was estimated in TDC using leave-one-out cross-validation (LOOCV). For the LOOCV, predicted values from "left-out" participants were obtained by taking the training data from all other healthy participants. This procedure was repeated until all healthy participants had a predicted value (Yip et al. 2019). Data from ASD participants were used for testing using the SVR trained in the TDC group (Fig. 1). The numeric value of the BCA indicates if brains appear younger (negative score) or older (positive score) than their ChA, and the numeric value specifies the magnitude of the difference (in years) between BCA and ChA (Luders et al. 2016). In line with previous studies, the predictive model (i.e., SVR) for BCA estimation was built with the hypothesis that no significant difference between BCA and ChA would appear in TDC (Franke et al. 2012, 2014).

Statistical Analysis

Two-sample *t*-tests were performed for the assessment of group differences in age, full-scale intelligence quotient (FIQ), and meanFD. The Kruskal–Wallis test was applied for the assessment of gender differences. Since both childhood and adolescence are periods of brain development during which the autistic brain has shown varying developmental patterns (McGovern and Sigman 2005; Courchesne et al. 2007), differences between BCA and ChA were examined with two-sample *t*-tests, and Pearson's correlation analyses between BCA and ChA were calculated separately in the two groups (ASD and TDC). The general linear model was used to compare the ΔAGE (i.e., the difference between BCA and ChA) between ASD and TDC separately in childhood and adolescence. Site, FIQ, sex, and head motion served as nuisance covariates. To examine whether the correspondence between BCA and ChA was influenced by head motion, Pearson's correlation analyses between distance (i.e., the distance of each dot from the linear fitting curve between BCA and ChA) and mean meanFD were further conducted.

Reproducibility Analysis

The robustness of our findings was firstly examined using only morphological information (i.e., 101 SEC and 6 SIC) and separately using the data from SDSU and NYU datasets. Next, in order

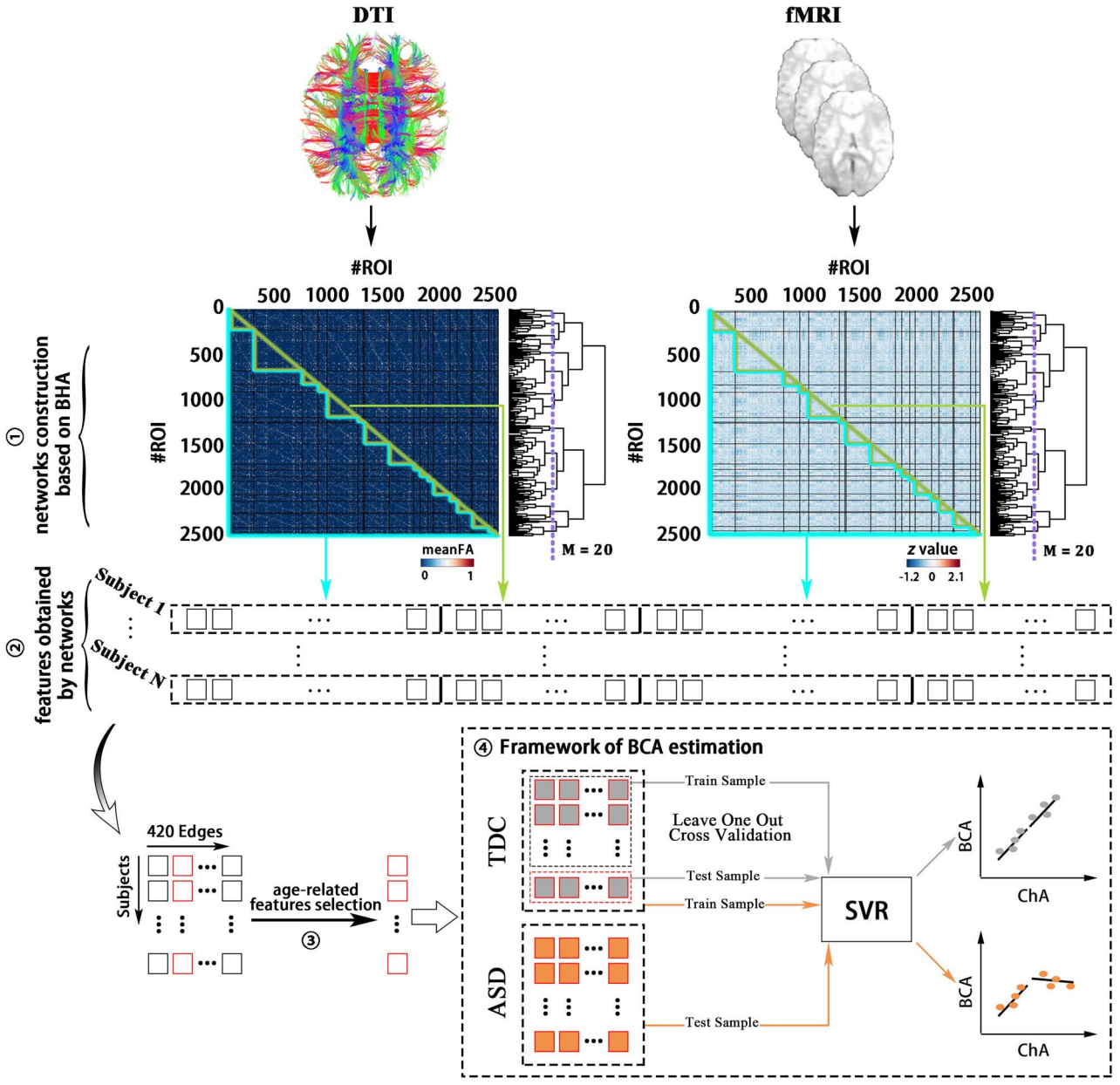

Figure 1. Methodological sketch. (1) Networks construction based on BHA: 2514 ROIs constitute 20 modules selected from the BHA, and 2514 × 2514 SC (FC) matrices for each participant were generated after image preprocessing. (2) Features obtained from networks: SIC, SEC, FIC, and FEC features were generated from the SC and FC networks. (3) Age-related feature selection: After the method RFECV and eliminating the effect of head motion, feature selection was performed. (4) Framework for BCA estimation: The BCA of each participant was generated by SVR and then compared with ChA. meanFA, mean of fractional anisotropy; BHA, Brain Hierarchical Atlas.

to test the robustness of our results against nuisance variances, BCA was estimated using an SVR model with the age-related features controlling for nuisance variances (i.e., site, FIQ, and sex). In addition, we used ridge regression (Chung et al. 2018) by minimizing the sum of squared prediction error and L2-norm regularization term to demonstrate that the reported findings are not model-dependent. Finally, to further examine the potential effect of global signal regression (GSR) on our findings, reproducibility analysis with GSR was conducted. Since the use of GSR in rs-fMRI studies has sparked a great deal of controversy and some investigators argue strongly against its use (Fox et al. 2009; Liu et al. 2017), the findings with GSR in this study are presented in Supplementary Information. For more details on reproducibility analyses, see Supplementary Information.

Results

Characterization of Age-Related Features

Of the 420 possible descriptors, 131 connections (Fig. 2 and Supplementary Fig. S1) had a greater SVR performance in the TDCs dataset and were used for BCA estimation. Among these

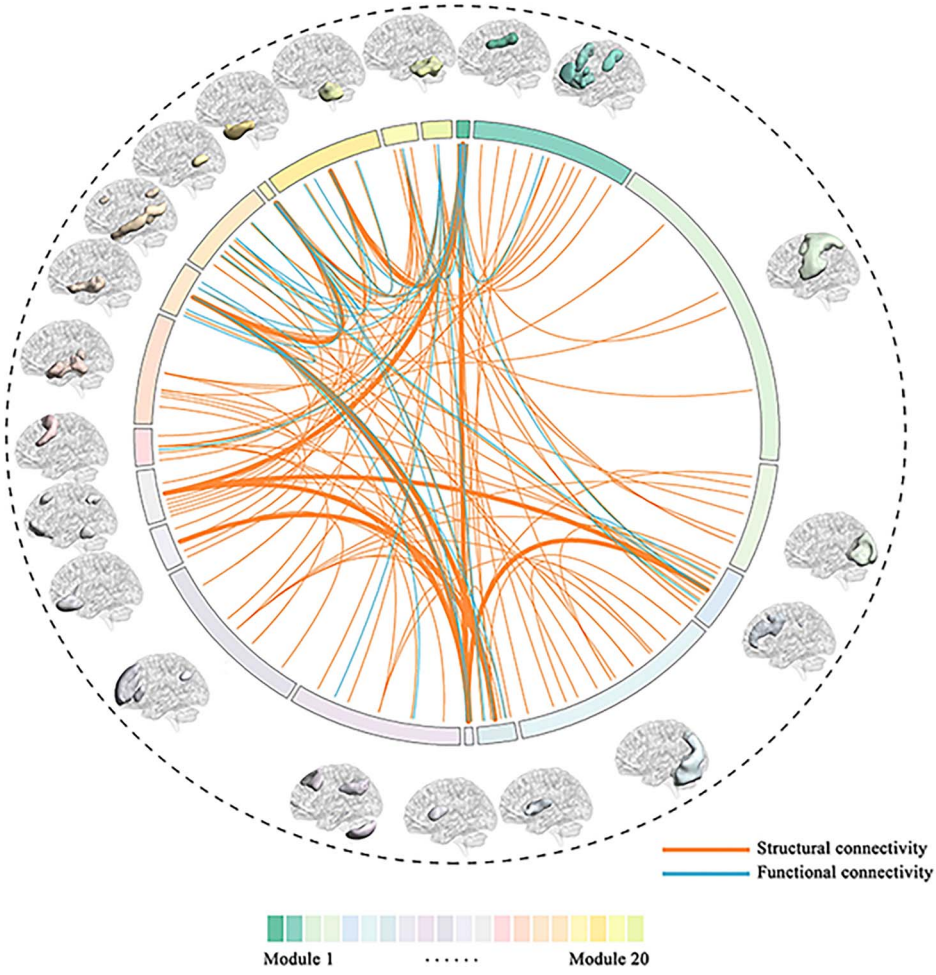

Figure 2. Selected features for BCA estimation in TDCs. A total number of 131 connections were selected as features for the estimation of BCA in TDCs. Twenty modules with different colors were used to calculate the different connectivity metrics FEC, FIC, SEC, and SIC. The arc length of each module is proportional to the number of ROIs within that module. Orange lines correspond to structural connections and blue lines to functional ones. The thickest lines represent the top 10 connections after ranking the weight in SVR.

connections, 101 connections were SEC, 6 SIC, 18 FEC, and 6 FIC (Supplementary Fig. S2). After ranking the weights of all connections in SVR, the 10 best descriptors included the thalamus (i.e., participating in modules 7 and 15), putamen (modules 7, 8, and 15), pallidum (modules 7 and 15), caudate nucleus (modules 7, 8, 11, and 12), nucleus accumbens (modules 7, 11, and 15), insula (module 15), hippocampus and amygdala (modules 15 and 18), anterior cingulate (modules 11 and 12), posterior cingulate (module 1), superior temporal gyrus (module 17), superior frontal gyrus (module 12), precentral gyrus (module 5), and lateral frontal orbital gyrus (modules 11 and 12). A complete anatomical description for all the 20 modules is given in Table S1 in Diez et al. (2015). Taken together, these descriptors were mainly involved in two circuits including the cortico-limbic-striatal (CLS) circuit and the fronto-insula-temporal (FIT) circuit, which play a central role in the BCA estimation. The core regions of the CLS circuit encompass temporal and frontal lobes, limbic structures (including a group of subcortical nuclei and cortical structures such as hippocampus and amygdala) and striatum, while the cortical regions of FIT circuit involve the orbitofrontal cortex, the medial temporal lobe (including the amygdala and hippocampus), and insula.

Relationships between BCA and ChA in Childhood and Adolescence in ASD versus TDC

Significant differences between BCA and ChA were observed in childhood (age range, 5–12 years) and adolescence (age range, 12–18 years) in ASD (Fig. 3, left). In childhood ASD, BCA was significantly higher than ChA (Fig. 3*a*). Moreover, BCA was positively correlated with ChA (Fig. 3*c*; $r = 0.56$, $P = 0.001$). In adolescent ASD, BCA was significantly lower than ChA (Fig. 3*a*), and notably BCA had no correlation with ChA (Fig. 3*c*; $r = 0.10$, $P = 0.69$). When performing the same analysis on the group of TDC, no significant differences were found in childhood or in adolescence (Fig. 3*b*). Moreover, TDC showed significant correlations between BCA and ChA in the two regimes (Fig. 3*d*; childhood: $r = 0.50$, $P = 0.004$; adolescence: $r = 0.75$; $P < 0.001$). Accordingly, ΔAGE of childhood ASD was significantly higher than that of childhood TDC, but ΔAGE of adolescent ASD was

smaller than that of adolescent TDC, though this decrement was not significant (Fig. 3e). This finding may be associated with atypical brain connections in ASD. No significant correlation between distance and mean FD was observed, suggesting that the correspondence between BCA and ChA is not trivially dependent on head motion (Supplementary Fig. S3).

Reproducibility of Findings

When repeating the entire analysis separately using the SDSU dataset (Supplementary Fig. S4), the NYU dataset with sample limitations (Supplementary Fig. S5), and only structural connections showing poor SVR performance of BCA estimation (i.e., 101 SEC and 6 SIC) (Supplementary Fig. S6), the same patterns of developmental trajectories in ASD can be observed. In addition, the same developmental patterns were also found separately by SVR using the features mitigating the effect of nuisance variances (i.e., site, FIQ, and sex) (Supplementary Fig. S7) and ridge regression (Supplementary Figs S8 and S9). Furthermore, the same developmental patterns were obtained from the data with GSR (Supplementary Fig. S10). Therefore, taken together, these analyses performed well with different conditions. Our findings are robust, showing that BCA was not significantly different from ChA in TDC, but they were differentiated in ASD (BCA > ChA in childhood and BCA < ChA in adolescence). For more details on reproducibility of findings, see Supplementary Information.

Discussion

To the best of our knowledge, this study is the first to identify discrepancies between ChA and BCA in ASD based on structure–function connectomics. ASD as compared with TDC is characterized by BCA being significantly higher than ChA in childhood, whereas BCA is significantly lower than ChA in adolescence. These results suggest that brain development in ASD seems to be accelerated in younger subjects but delays with increasing age (Fig. 4). Measurements of BCA on single subject might serve as potential biomarkers for characterizing brain developmental trajectories in ASD.

Methodological Considerations

Recent studies have measured brain age based on biological information, but few have combined SC and FC features to implement the estimation (Franke et al. 2012; Gaser et al. 2013; Cole et al. 2015). Combined features are of crucial importance, as structural connections provide support to functional connections, while functional connections exert effects on the plasticity of structural connections in the course of brain development (Hermundstad et al. 2013). Liem et al. (2017) have reported that the error of brain age estimation was 4.29 years by combining morphological information with FC. Bonifazi et al. (2018) have achieved high performance of brain age by combining SC and FC metrics at different spatial scales along a hierarchical tree. Here, we have shown that a combination of SC and FC metrics might allow for the sensitive detection of aberrant patterns in brain development.

Although the functional and structural datasets were obtained from the same subject, SC and rsFC networks were acquired by using different prior structural and functional templates, respectively (Zhang et al. 2011; Hermundstad et al. 2013; Jimenez-Marin et al. 2019). Thus, the two modalities consist of two separate and autonomous datasets related to different physical and physiological mechanisms. However, specific functional connections between distinct regions are necessarily constrained by the underlying wiring structure, and functional connections rely on existing structural ones (Hermundstad et al. 2013). In the current study, to ensure correspondence between function and structure, the brain was partitioned into 20 modules relevant for both structure and function, as shown in Diez et al. (2015). In addition, linear SVR was selected to avoid the potential effect of overfitting between brain connectomics and ChA, and ridge regression was applied to demonstrate that our results are not model-dependent.

The CLS Circuit Has a Major Role in BCA Estimation

Our findings demonstrate that the CLS circuit plays a major role in BCA estimation. CLS involves temporal and frontal lobes, limbic structures such as the hippocampus and amygdala, and striatum (Jiang et al. 2017). CLS is well known to play an important role in emotion processing (Cardinal et al. 2002), during which cortical regions such as the frontal lobe integrate signals received from limbic structures to be sent back to limbic structures and striatum (Braun 2011). Importantly, emotion processing ability improves with age and, when it fails, pathological social behaviors can emerge (Custrini and Feldman 1989). In the transition from childhood into adolescence, children's capacity to regulate their emotion increases with age and is seriously affected by social–contextual factors (Gnepp and Hess 1986). Our findings of BCA and ChA differences in ASD indicate that the functioning of the CLS circuit in regulating emotion processing is one that may be altered when autistic children age.

The FIT Circuit Is Also Relevant for the BCA Estimation

Our findings also show that the insula participates in BCA estimation, together with the orbitofrontal cortex and the medial temporal lobe (including the amygdala and hippocampus) form the FIT circuit (Gleichgerrcht et al. 2010). The FIT circuit is responsible for decision-making (Gleichgerrcht et al. 2010), an extremely complex human behavior involving stimulus encoding, action selection, and expected reward (Gleichgerrcht et al. 2010). Accumulating evidence suggests that the FIT circuit is affected in brain neurodegenerative diseases such as frontotemporal dementia, Parkinson disease, and Alzheimer's disease (Taylor et al. 1986; Rahman et al. 1999; Torralva et al. 2000). Importantly, Mann et al. (1989) and Cauffman et al. (2010) showed that young adolescents had impairment in decision-making as compared with older individuals, suggesting that developmental differences affect decision-making performance, particularly under situations of emotional engagement and uncertain outcome. Our findings showing that differences between BCA and ChA in ASD, in part coming from the FIT circuit, might underlie altered decision-making ability in autistic developing brains.

Simultaneous Structure–Function Contribution to BCA Estimation

Our findings demonstrate that some brain regions have a critical contribution to BCA estimation, as their connectivity contributed simultaneously for both structure and function (purple

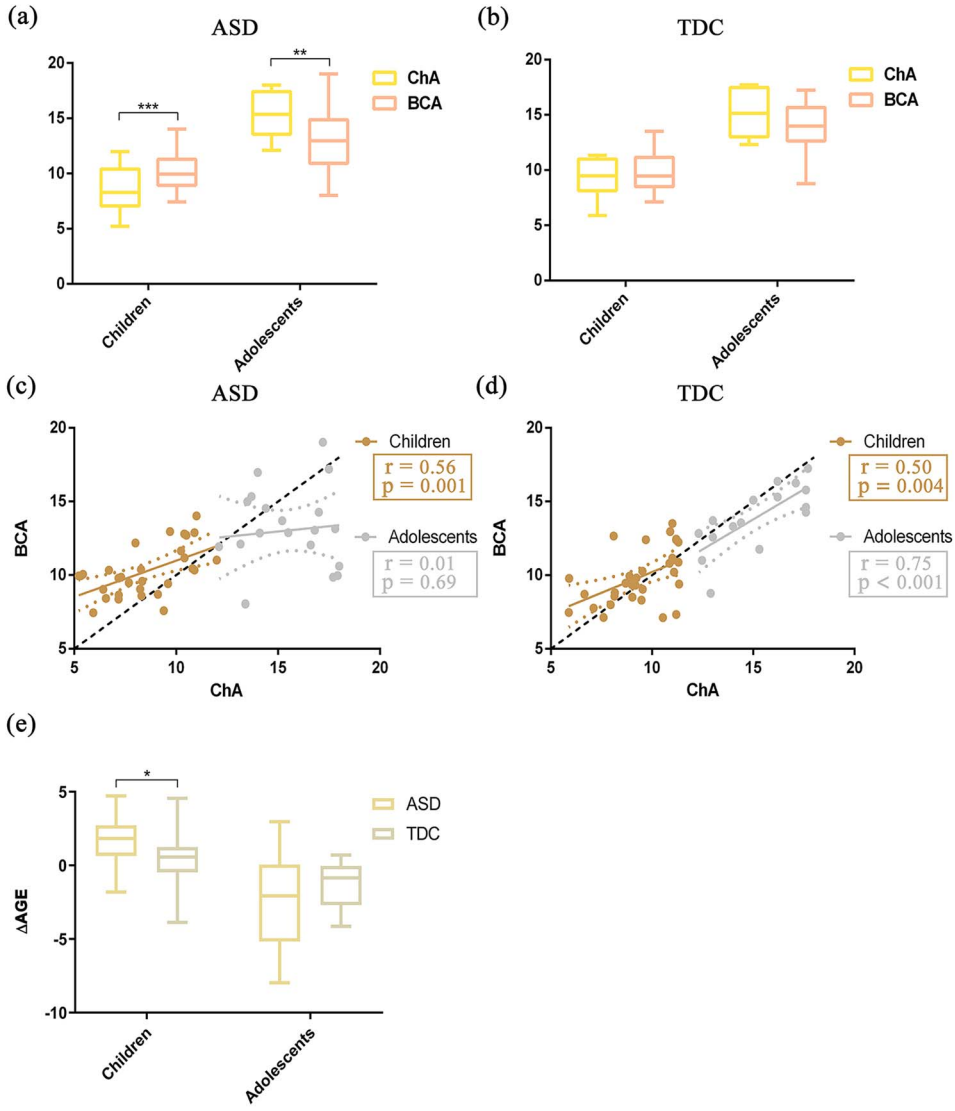

Figure 3. Relationships between BCA and ChA and differences of ΔAGE in childhood and adolescence for the two groups ASD and TDC (childhood, age 5–12 years; adolescence, age 12–18 years). (*a*) Group differences between BCA and ChA in childhood and adolescent ASD. Yellow represents ChA and red represents BCA. Error bars indicate the range of values. (*b*) Similar to (*a*) but for TDC. (*c*) Correlation between BCA and ChA in the two regimes: childhood (gold) and adolescence (silver). (*d*) Similar to (*c*), but for TDC. Gold represents childhood and silver represents adolescence. The diagonal dashed line represents the line BCA = ChA. (*e*) Group difference of ΔAGE between ASD and TDC in childhood. Beige represents childhood ASD and gray represents childhood TDC. ΔAGE represents the difference of BCA from ChA (i.e., ΔAGE = BCA − ChA) (left). Similar to the left (*e*), but for adolescence (right). $^{*}P < 0.05$, $^{**}P < 0.01$, $^{***}P < 0.001$ after two-sample *t*-tests.

in Supplementary Fig. S2). These areas included basal ganglia, superior parietal gyrus, superior frontal gyrus, postcentral gyrus, insula, cerebellum, and the limbic system. Our results suggest that both SC and FC of these areas play an important role in the autistic brains and highlight the critical role of SC and FC in the pathophysiological mechanisms underlying ASD. In the current study, white matter SC obtained from DTI data using the fiber tracking strategy, critically contributed to the SVR performance for BCA estimation. Additionally, many previous studies have reported that white matter carries functional information and highlights its neurobiological relevance in the brain, similar to gray matter (Ji et al. 2017, 2019; Peer et al. 2017; Li et al. 2019). Thus, future studies using white matter structure together with its functional information are necessary to broaden our understanding of the neurobiological developmental underpinnings of the autistic brain.

Trajectories of BCA in Childhood and Adolescence in ASD

We found discrepancies of brain development deviating from normal aging in childhood and adolescence in ASD concerning SC and FC. Specifically, BCA was significantly higher than ChA in childhood ASD, while BCA was significantly lower than ChA in adolescent ASD. These findings are in agreement with previous results of age-related changes in anatomical and functional

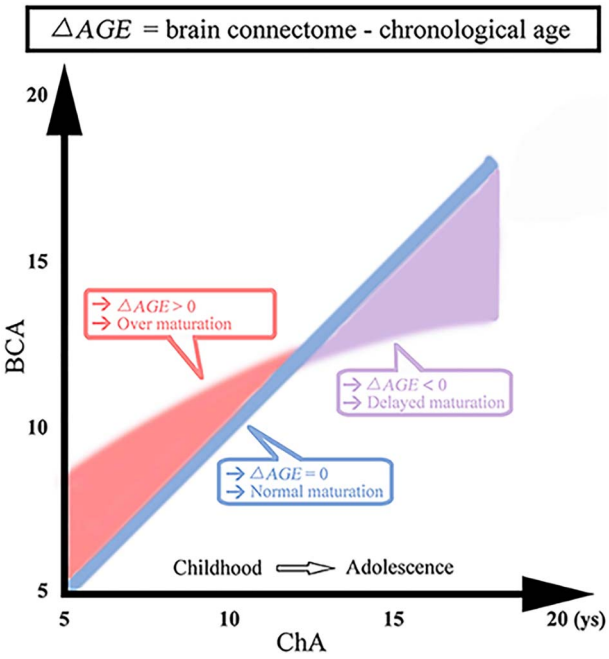

Figure 4. Difference between BCA and ChA. Blue line, BCA and ChA are highly correlated in TDC. Red regime: BCA was higher than ChA in childhood ASD. Purple regime: BCA was lower than ChA in adolescent ASD. ys, years.

connectivity showing that children with ASD have increased FA (Billeci et al. 2012) and, in contrast, adolescents with ASD do have reduced FA (Keller et al. 2007). Additionally, Uddin et al. (2013) showed increased FC in children with ASD and reduced FC in older individuals. Moreover, overgrowth processes (including an excessive number of axonal connections and premature myelination) among children with ASD and degenerative processes (including loss of connections and neuron loss) among adolescents with ASD is an established neurobiological finding (Courchesne et al. 2004, 2007). These results showing two regimes of brain maturation in ASD agree with our current results and further suggest that such a transition might occur at preadolescence. Recently, some studies have characterized ASD as a disorder emerging at a critical period, reporting excessive plasticity occurring at the wrong times, resulting from noisy and unstable processing (Rubenstein and Merzenich 2003; Uddin et al. 2013). Therefore, our results exhibiting aberrant BCA might indicate higher levels of plasticity in childhood (excessive plasticity) and the opposite in adolescence (delayed plasticity). Early identification of BCA could potentially improve clinical outcomes in ASD through early treatment or prophylaxis.

Limitations

Our findings should be interpreted in light of some limitations. First, the sample size is relatively small due to the requirement of multimodal data (fMRI and DTI) and age range (5–18 years). Larger sample sizes are required to replicate and confirm our results. Second, the healthy sample dataset of TDC in this study was utilized to train the model and uncover age-related brain connectivity providing useful information of normal aging patterns, rather than an independent healthy sample dataset. We were unable to obtain an independent dataset to train the model. However, we performed a series of reproducibility analyses to investigate the robustness of our findings, which could alleviate the risk of overfitting in the current study. Future work should aim to train models using completely independent datasets. Moreover, following previous work (Lawrence et al. 2019), longitudinal (rather than cross-sectional) studies are needed for the validation of the aberrant developmental trajectories found in ASD.

Conclusion

We found that BCA was significantly higher than ChA in childhood ASD, while BCA was significantly lower than ChA in adolescent ASD. These results suggest that discrepancies between BCA and ChA may be attributed to abnormal developmental trajectories in ASD and demonstrate that, compared with TDCs, ASD exhibits accelerated brain development in youth followed by a delay after preadolescence. Furthermore, we suggest that BCA from multimodal imaging data is a potentially useful biomarker for understanding atypical neurodevelopmental patterns in ASD.

Supplementary Material

Supplementary material is available at *Cerebral Cortex* online.

Notes

We are grateful to all the participants and their guardians in this study.

Funding

National Natural Science Foundation of China (Nos. 61533006, 61673089, 81871432, U1808204); Sichuan Science and Technology Program (2018TJPT00160, 2019YJ0180); Fundamental Research Funds for the Central Universities (Nos. 2672018ZYGX2018J079, ZYGX2019Z017); Key Project of Research and Development of Ministry of Science and Technology (2018AAA0100705); Ikerbasque and from Ministerio Economia, Industria y Competitividad (Spain) and FEDER (grant DPI2016-79874-R to J.M.C., grant SAF2015-69484-R to P.B.); Department of Economical Development and Infrastructure of the Basque Country (Elkartek Program, KK-2018/00032 to J.M.C.); National Institute of Mental Health (R01MH107549 to L.Q.U.); National Natural Science Foundation of China (61901129 to H.C.). *Conflict of Interest*: The authors declare no conflict of interest.

References

American Psychiatric Association. 2013. *Diagnostic and Statistical Manual of Mental Disorders (DSM-5®)*. Washington, DC: American Psychiatric Publishing.

Billeci L, Calderoni S, Tosetti M, Catani M, Muratori F. 2012. White matter connectivity in children with autism spectrum disorders: a tract-based spatial statistics study. *BMC Neurol*. 12:148.

Bonifazi P, Erramuzpe A, Diez I, Gabilondo I, Boisgontier MP, Pauwels L, Stramaglia S, Swinnen SP, Cortes JM. 2018. Structure–function multi-scale connectomics reveals a major role of the fronto-striato-thalamic circuit in brain aging. *Hum Brain Mapp*. 39:4663–4677.

Braun K. 2011. The prefrontal-limbic system: development, neuroanatomy, function, and implications for socioemotional development. *Clin Perinatol*. 38:685–702.

Cardinal RN, Parkinson JA, Hall J, Everitt BJ. 2002. Emotion and motivation: the role of the amygdala, ventral striatum, and prefrontal cortex. *Neurosci Biobehav Rev*. 26:321–352.

Cauffman E, Shulman EP, Steinberg L, Claus ED, Banich MT, Graham S, Woolard JL. 2010. Age differences in affective decision making as indexed by performance on the Iowa gambling task. *Dev Psychol*. 46:193–207.

Chung Y, Addington J, Bearden CE, Cadenhead K, Cornblatt B, Mathalon DH, McGlashan T, Perkins D, Seidman LJ, Tsuang M. 2018. Use of machine learning to determine deviance in neuroanatomical maturity associated with future psychosis in youths at clinically high risk. *JAMA Psychiatry*. 75:960–968.

Cole JH, Leech R, Sharp DJ, Initiative ADN. 2015. Prediction of brain age suggests accelerated atrophy after traumatic brain injury. *Ann Neurol*. 77:571–581.

Courchesne E, Pierce K, Schumann CM, Redcay E, Buckwalter JA, Kennedy DP, Morgan J. 2007. Mapping early brain development in autism. *Neuron*. 56:399–413.

Courchesne E, Redcay E, Kennedy DP. 2004. The autistic brain: birth through adulthood. *Curr Opin Neurol*. 17:489–496.

Craddock RC, James GA, Holtzheimer PE, Hu X, Mayberg HS. 2012. A whole brain fMRI atlas generated via spatially constrained spectral clustering. *Hum Brain Mapp*. 33:1914–1928.

Custrini RJ, Feldman RS. 1989. Children's social competence and nonverbal encoding and decoding of emotions. *J Clin Child Psychol*. 18:336–342.

Di Martino A, O'connor D, Chen B, Alaerts K, Anderson JS, Assaf M, Balsters JH, Baxter L, Beggiato A, Bernaerts S. 2017. Enhancing studies of the connectome in autism using the autism brain imaging data exchange II. *Sci Data*. 4:1–15.

Di Martino A, Yan C-G, Li Q, Denio E, Castellanos FX, Alaerts K, Anderson JS, Assaf M, Bookheimer SY, Dapretto M. 2014. The autism brain imaging data exchange: towards a large-scale evaluation of the intrinsic brain architecture in autism. *Mol Psychiatry*. 19:659–667.

Diez I, Bonifazi P, Escudero I, Mateos B, Muñoz MA, Stramaglia S, Cortes JM. 2015. A novel brain partition highlights the modular skeleton shared by structure and function. *Sci Rep*. 5:10532.

Dosenbach NUF, Binyam N, Cohen AL, Fair DA, Power JD, Church JA, Nelson SM, Wig GS, Vogel AC, Lessov-Schlaggar CN. 2010. Prediction of individual brain maturity using fMRI. *Science*. 329:1358–1361.

Drucker H, Burges CJ, Kaufman L, Smola AJ, Vapnik V. 1997. Support vector regression machines. *Adv Neural Inf Proces Syst*. 9:155–161.

Ecker C, Bookheimer SY, Murphy D. 2015. Neuroimaging in autism spectrum disorder: brain structure and function across the lifespan. *Lancet Neurol*. 14:1121–1134.

Fox MD, Zhang D, Snyder AZ, Raichle ME. 2009. The global signal and observed anticorrelated resting state brain networks. *J Neurophysiol*. 101:3270–3283.

Franke K, Luders E, May A, Wilke M, Gaser C. 2012. Brain maturation: predicting individual BrainAGE in children and adolescents using structural MRI. *NeuroImage*. 63:1305–1312.

Franke K, Ristow M, Gaser C. 2014. Gender-specific impact of personal health parameters on individual brain aging in cognitively unimpaired elderly subjects. *Front Aging Neurosci*. 6:94.

Gaser C, Franke K, Klöppel S, Koutsouleris N, Sauer H, Initiative ADN. 2013. BrainAGE in mild cognitive impaired patients: predicting the conversion to Alzheimer's disease. *PLoS One*. 8:e67346.

Gleichgerrcht E, Ibanez A, Roca M, Torralva T, Manes F. 2010. Decision-making cognition in neurodegenerative diseases. *Nat Rev Neurol*. 6:611–623.

Gnepp J, Hess DLR. 1986. Children's understanding of verbal and facial display rules. *Dev Psychol*. 22:103–108.

Guyon I, Weston J, Barnhill S, Vapnik V. 2002. Gene selection for cancer classification using support vector machines. *Mach Learn*. 46:389–422.

Hermundstad AM, Bassett DS, Brown KS, Aminoff EM, Clewett D, Freeman S, Frithsen A, Johnson A, Tipper CM, Miller MB. 2013. Structural foundations of resting-state and task-based functional connectivity in the human brain. *Proc Natl Acad Sci*. 110:6169–6174.

Ji GJ, Liao W, Chen F-F, Zhang L, Wang K. 2017. Low-frequency blood oxygen level-dependent fluctuations in the brain white matter: more than just noise. *Sci Bull*. 62:656–657.

Ji GJ, Ren C, Li Y, Sun J, Liu T, Gao Y, Xue D, Shen L, Cheng W, Zhu C. 2019. Regional and network properties of white matter function in Parkinson's disease. *Hum Brain Mapp*. 40:1253–1263.

Jiang X, Dai X, Edmiston EK, Zhou Q, Xu K, Zhou Y, Wu F, Kong L, Wei S, Zhou Y. 2017. Alteration of cortico-limbic-striatal neural system in major depressive disorder and bipolar disorder. *J Affect Disord*. 221:297–303.

Jimenez-Marin A, Rivera D, Boado V, Diez I, Labayen F, Garrido I, Ramos-Usuga D, Benito-Sanchez I, Rasero J, Cabrera-Zubizarreta A. 2019. Brain connectivity and cognitive functioning in individuals six months after multiorgan failure. *Neuroimage Clin*. 25:102–137.

Keller TA, Kana RK, Just MA. 2007. A developmental study of the structural integrity of white matter in autism. *Neuroreport*. 18:23–27.

Kleinhans NM, Pauley G, Richards T, Neuhaus E, Martin N, Corrigan NM, Shaw DW, Estes A, Dager SR. 2012. Age-related abnormalities in white matter microstructure in autism spectrum disorders. *Brain Res*. 1479:1–16.

Lawrence KE, Hernandez LM, Bookheimer SY, Dapretto M. 2019. Atypical longitudinal development of functional connectivity in adolescents with autism spectrum disorder. *Autism Res*. 12:53–65.

Li J, Biswal BB, Wang P, Duan X, Cui Q, Chen H, Liao W. 2019. Exploring the functional connectome in white matter. *Hum Brain Mapp*. 40:4331–4344.

Liem F, Varoquaux G, Kynast J, Beyer F, Masouleh SK, Huntenburg JM, Lampe L, Rahim M, Abraham A, Craddock RC. 2017. Predicting brain-age from multimodal imaging data captures cognitive impairment. *NeuroImage*. 148:179–188.

Liu TT, Nalci A, Falahpour M. 2017. The global signal in fMRI: nuisance or information? *NeuroImage*. 150:213–229.

Luders E, Cherbuin N, Gaser C. 2016. Estimating brain age using high-resolution pattern recognition: younger brains in long-term meditation practitioners. *NeuroImage*. 134: 508–513.

Mann L, Harmoni R, Power C. 1989. Adolescent decision-making: the development of competence. *J Adolesc*. 12:265–278.

McGovern CW, Sigman M. 2005. Continuity and change from early childhood to adolescence in autism. *J Child Psychol Psychiatry*. 46:401–408.

Nomi JS, Uddin LQ. 2015. Developmental changes in large-scale network connectivity in autism. *NeuroImage Clin*. 7:732–741.

Pang Y, Chen H, Chen Y, Cui Q, Wang Y, Zhang Z, Lu G, Chen H. 2019. Extraversion and neuroticism related to topological efficiency in white matter network: an exploratory study using diffusion tensor imaging tractography. *Brain Topogr*. 32:87–96.

Peer M, Nitzan M, Bick AS, Levin N, Arzy S. 2017. Evidence for functional networks within the human brain's white matter. *J Neurosci*. 37:6394–6407.

Rahman S, Sahakian BJ, Hodges JR, Rogers RD, Robbins TW. 1999. Specific cognitive deficits in mild frontal variant frontotemporal dementia. *Brain*. 122:1469–1493.

Rubenstein J, Merzenich MM. 2003. Model of autism: increased ratio of excitation/inhibition in key neural systems. *Genes Brain Behav*. 2:255–267.

Schnack HG, Van Haren NE, Nieuwenhuis M, Hulshoff Pol HE, Cahn W, Kahn RS. 2016. Accelerated brain aging in schizophrenia: a longitudinal pattern recognition study. *Am J Psychiatry*. 173:607–616.

Silk TJ, Wood AG. 2011. Lessons about neurodevelopment from anatomical magnetic resonance imaging. *J Dev Behav Pediatr*. 32:158–168.

Taylor AE, Saintcyr JA, Lang AE. 1986. Frontal lobe dysfunction in Parkinson's disease. The cortical focus of neostriatal outflow. *Brain*. 109:845–883.

Torralva T, Dorrego F, Sabe L, Chemerinski E, Starkstein SE. 2000. Impairments of social cognition and decision making in Alzheimer's disease. *Int Psychogeriatr*. 12:359–368.

Uddin LQ, Supekar K, Menon V. 2013. Reconceptualizing functional brain connectivity in autism from a developmental perspective. *Front Hum Neurosci*. 7:458.

Yan C, Zang Y. 2010. DPARSF: a MATLAB toolbox for "pipeline" data analysis of resting-state fMRI. *Front Syst Neurosci*. 4:13.

Yip SW, Scheinost D, Potenza MN, Carroll KM. 2019. Connectome-based prediction of cocaine abstinence. *Am J Psychiatry*. 176:156–164.

Zhang Z, Liao W, Chen H, Mantini D, Ding J-R, Xu Q, Wang Z, Yuan C, Chen G, Jiao Q. 2011. Altered functional–structural coupling of large-scale brain networks in idiopathic generalized epilepsy. *Brain*. 134:2912–2928.

Zimmermann J, Ritter P, Shen K, Rothmeier S, Schirner M, McIntosh AR. 2016. Structural architecture supports functional organization in the human aging brain at a regionwise and network level. *Hum Brain Mapp*. 37:2645–2661.